

Precipitation of copper and chromium impurities in lanthanum magnesium aluminate crystals during thermochemical reduction

C. Ballesteros

Departamento de Física de Materiales, Universidad Complutense, 28040 Madrid, Spain

R. González

Departamento de Ingeniería, Escuela Politécnica Superior, Universidad Carlos III, 28913 Leganés (Madrid), Spain

Y. Chen*

Solid State Division, Oak Ridge National Laboratory, Oak Ridge, Tennessee 37831-6031

M. R. Kokta

Union Carbide Corporation, Washougal, Washington 98671

(Received 9 March 1992)

Thermochemical reduction at high temperatures has been performed on chromium-doped lanthanum magnesium aluminate crystals. Analytical transmission-electron-microscopy and optical-absorption techniques were used to characterize the crystals. Copper impurities inherently present in the crystals began to aggregate and form Cu-rich particles at 1500 K near the surface region. Below 1870 K there was no evidence of chromium precipitates being formed. However, Cr-rich particles were formed at 2020 K. The distribution of the precipitates was very inhomogeneous and the precipitates were also concentrated near the surface region.

I. INTRODUCTION

The optical, mechanical, and electrical properties of a refractory oxide crystal are affected by its past thermal history. For example, when the oxide crystals are heated in a reducing atmosphere, as a general feature, oxygen vacancies and/or precipitate phases are formed.¹⁻⁸ The precipitates are usually metallic particles. The small particles with diameters in the range of 1–200 nm in ionic crystals lead to important changes in these properties.⁹ These particles are usually identified by analytical electron microscopy. Typically they give rise to characteristic broad extinction bands, due to Mie scattering. Their shape, structure, and properties are strongly influenced by the crystal structure of the host lattice and the conditions of the heat treatments.

Lanthanum magnesium aluminate, $\text{LaMgAl}_{11}\text{O}_{19}$ (or LMA), has the hexagonal magnetoplumbite structure.¹⁰ It is a promising host for optical devices and as a result has been the subject for recent optical and magnetic-resonance studies.¹¹⁻¹⁶ As in other oxide crystals, its optical properties are strongly affected by its past thermal history. In the present study, we subject Cr-doped LMA crystals to thermochemical reduction at high temperatures and examine the change in the optical absorption. The cause of the change is studied by transmission electron microscopy.

II. EXPERIMENTAL PROCEDURES

The lanthanum magnesium aluminate was grown by the Czochralski pulling technique. The charge was prepared by mixing constituent oxides in appropriate ra-

tios to yield crystals with 0.2 at. % of Cr^{3+} in the $\text{LaMgAl}_{11}\text{O}_{12}$ formula. All constituent oxides were of five 9's purity level. Special precautions were taken in the treatment of the lanthanum oxide. The La_2O_3 was fired for 12 h at 1373 K, cooled in a desiccator, and weighed out immediately in order to prevent H_2O and CO_2 reabsorption before weighing.

The mixed oxides were pressed in a isostatic press and charged into a 76×76-mm iridium crucible. The crucible was placed into a coupling coil of 50 kW, 10 kHz radio-frequency (RF) generator. The coil crucible assembly was insulated with zirconium oxide ceramic tubes and placed in a bell-jar enclosure. This enclosure was used in order to maintain a precise oxygen concentration in the ambient atmosphere.

The charge was melted at approximately 2273 K and the LMA seed of "a" orientation used for seeding. The actual growth was carried out at a pulling rate of 0.38 mm/h. The seed was rotated at a constant rate of 15 rpm.

The crystal was grown to a nominal 38-mm diameter using an automatic diameter control system. The control system utilizes the signal from the load cell, which reacts to changes of the weight of the growing crystal. The crystal growth of high optical quality LMA crystal does not pose any special difficulties and does not deviate from any standard techniques used for the growth of optical crystals.

Thermochemical reduction (TCR) was performed primarily in a Lindberg furnace, and for temperatures above 1900 K in an Astro furnace, model 1000-2560 FP, with the sample enclosed in a graphite chamber with flowing oxygen-free nitrogen gas. The duration of TCR at each

temperature was 1 h, unless otherwise indicated.

Optical absorption measurements were made with a Perkin-Elmer Lambda-9 spectrophotometer. The specimens for the optical studies were thinned down initially on silicon carbide paper and subsequently polished with diamond paste. The sample surface was perpendicular to the *c* axis. Following TCR, optical absorption measurements were made. At some points, small pieces of the sample were cut off to be used for transmission electron microscopy (TEM). These specimens were prepared using standard techniques, first ground and then thinned down using argon ion-milling in a liquid-nitrogen-cooled holder.

X-ray microanalysis and diffraction studies of individual precipitates were carried out using a Philips 420 and a Jeol 2000 FX analytical electron microscopes. The electron optics of the instruments allow fine electron probes to be readily obtained. Thus it was possible to obtain diffraction information from areas as small as 10 nm in diameter.

III. RESULTS AND DISCUSSION

Optical absorption and analytical transmission electron microscopy were used as complementary techniques to investigate chromium and defect formation in the crystals. The optical measurements monitor the impurities and vacancies in solution. In the virgin crystal chromium was present exclusively as substitutional Cr^{3+} ions, absorbing at 420 and 570 nm.¹⁷ Upon TCR at increasingly higher temperatures, changes were observed in the optical-absorption spectra. TEM monitors extended defects at various stages of TCR, particularly impurity aggregation. Two stages of impurity aggregation were observed. The first stage involved the emergence of newly formed defects and precipitation of copper impurities, which were apparently present in the virgin crystals. The Cu-rich precipitates were concentrated near the surface region and were characterized by a dark coloration, presumably due to Mie scattering. The temperature range was between 1500 and 1900 K. No chromium impurities were detected in these precipitates. The second stage occurred above 1900 K and involved precipitates of the chromium dopant. The results of the two stages are presented as follows.

A. Stage 1: Vacancy formation and Copper precipitation

There appeared to be no activities in the crystals below 1500 K that led to changes observable by optical absorption or TEM measurements. Between 1500 and 1870 K changes were observed: In the bulk material optical absorption increased in the ultraviolet region, and in the surface region a dark coloration emerged. The surface region was investigated by TEM. For the optical measurements of the bulk material, the thin layers of coloration on each side were removed by polishing.

The optical-absorption spectra of a LMA:Cr crystal before and after isochronal TCR are shown in Fig. 1. From 1500-K to ≥ 1870 -K absorption in the ultraviolet region increased monotonically: An absorption peak at 270 nm became more intense with an increase in the TCR

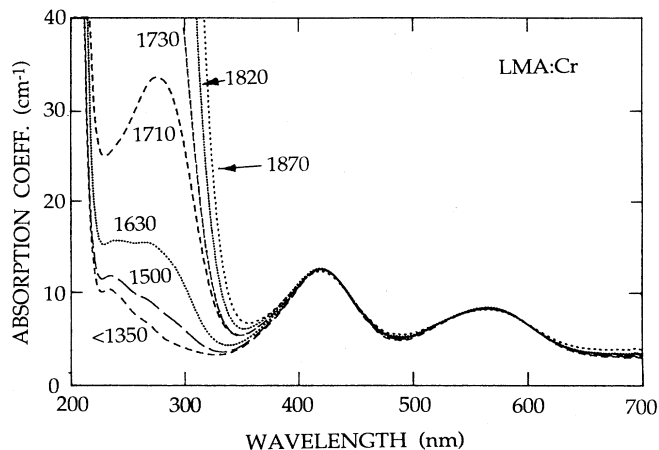


FIG. 1. Optical-absorption coefficient vs wavelength for a LMA:Cr crystal thermochemically reduced up to a temperature of 1820 K.

temperature. The spectra in the visible and infrared region remained the same in this temperature range, indicating that the concentration of Cr^{3+} ions remained constant. Even though Fe is a common impurity in most oxides, the absorption at 270 nm is clearly not due to a Fe^{3+} charge-transfer band. There are three reasons: (1) The absorption peaks and the full width at half maximum (FWHM) are different. The Fe^{3+} charge-transfer band peaks at 260 nm and has a FWHM of about 0.88 eV, whereas the absorption band in the TCR crystal peaks at 270 nm and has a FWHM of about 1.2 eV. (2) Any Fe^{3+} concentration should diminish rather than increase because a TCR process reduces the valence of the Fe impurity. (3) The absorption did not saturate, but continued to increase with the TCR temperature. The monotonic increase with temperature is a strong indication that intrinsic defects were being formed and not an indication that a change in valence was taking place. In analogy with other oxides, we propose that, as a result of TCR-induced nonstoichiometry, the absorption band at 270 nm is associated with anion vacancies, or an anion-vacancy complex.

Concomitant with the emergence of the 270-nm band at 1500 K was the appearance of a dark coloration at the surface region. It was observed that as the TCR temperature increases, the dark surface layer became thicker and darker. TEM investigation was made for the dark region as well as the bulk material. The dark regions were characterized by a dilute concentration of widely separated precipitates with an average size of 14 nm. Figure 2 shows a micrograph with two typical precipitates. X-ray fluorescence experiments using the small convergent probe indicates that the precipitates were Cu rich, presumably Cu particles. Occasionally a small concentration of either Ti or Mo was also observed in the precipitates. No Cr-rich precipitates were observed, consistent with optical-absorption measurements that there was no loss of substitutional Cr^{3+} ions. Figure 3 illustrates a typical x-ray fluorescence spectrum from a Cu-rich precipitate. Due to both the low intensity of the pre-

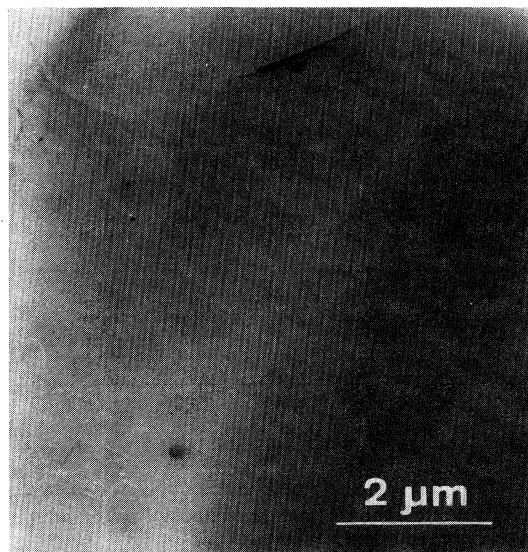


FIG. 2. Bright-field transmission-electron microscopy of precipitates in LMA:Cr crystal thermochemically reduced at 1500 K.

precipitate spots and the high number of matrix spots, microdiffraction patterns from the precipitates could not be obtained. Precipitates were only detected in regions close to the surfaces. Therefore it is reasonable to attribute the dark coloration to Mie scattering from the Cu-rich precipitates. In general, the formation of cation-rich precipitates due to TCR tends to initiate at the surface, and the present observation seems to be no exception.

The simultaneous emergence of vacancies and precipitates is not unusual. In fact, there are many systems in which TCR results in the formation of anion vacancies and that these vacancies are a necessary precursor to the formation of impurity metallic precipitates.^{1,3,5-7}

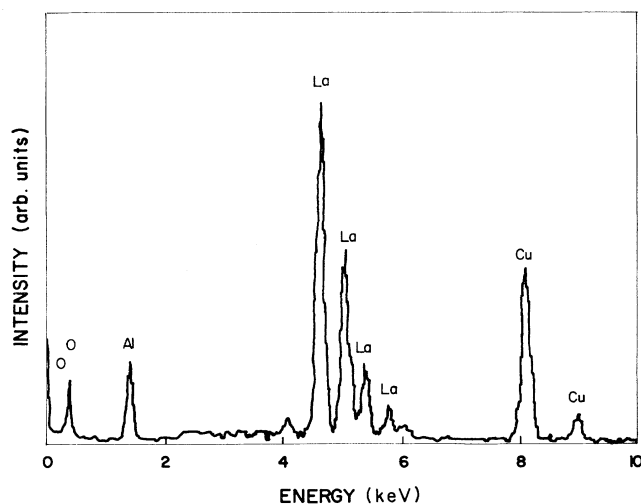


FIG. 3. X-ray fluorescence spectrum of a copper-rich precipitate in LMA:Cr crystal thermochemically reduced at 1500 K.

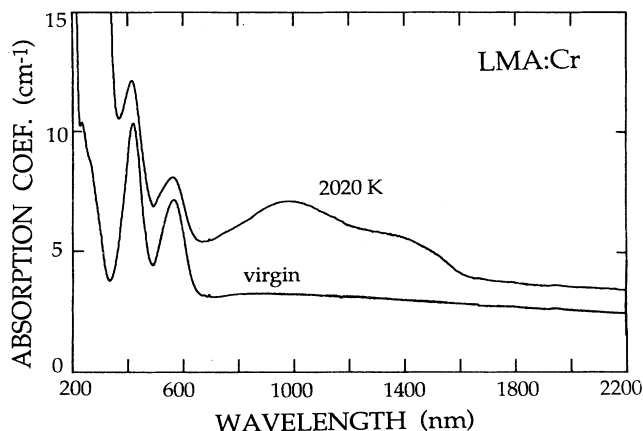


FIG. 4. Optical-absorption spectra for a virgin LMA:Cr crystal (bottom), and a LMA:Cr crystal after thermochemical reduction at 2020 K.

B. Stage 2: Chromium precipitation

Aggregation of chromium impurities began to take place at a temperature above 1870 K. The supporting evidences are the optical absorption and the TEM measurements. A crystal of LMA:Cr was thermochemically reduced at 2020 K for 2 h. The spectra before and after the TCR are shown in Fig. 4. Changes in the three wavelength regions are noted: (1) In the ultraviolet region the absorption continued to increase, an obvious extension from the increasing trend noted in Fig. 1. Such strong temperature dependence is indeed consistent with the formation of anion vacancies associated with nonstoichiometry resulting from the TCR.^{5-7,18,19} These vacancies are presumably the precursors for the formation of the metallic precipitates. (2) In the visible region the absorption was dominated by the tail end of the ultraviolet-

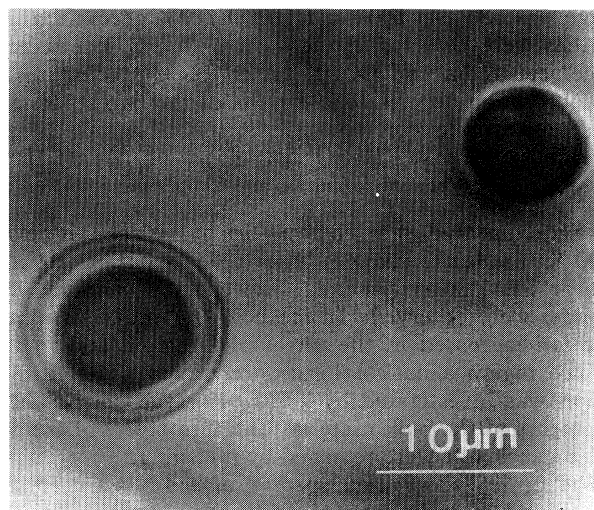


FIG. 5. Bright-field transmission-electron microscopy of precipitates in a LMA:Cr crystal thermochemically reduced at 2020 K.

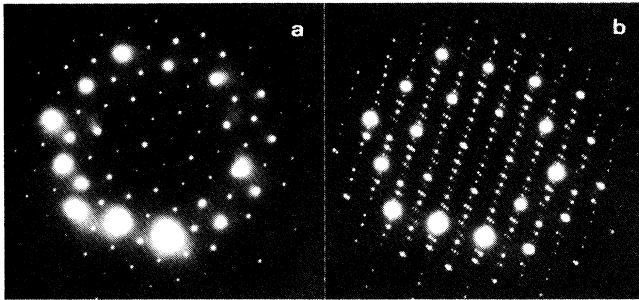


FIG. 6. Selected-area-diffraction patterns of (a) the matrix, and (b) a precipitate in a LMA:Cr crystal thermochemically reduced at 2020 K.

let absorption. Nevertheless, it is apparent that the two Cr^{3+} peaks (420 and 570 nm) had diminished, indicating that there was a loss of the dopant ions. (3) In the near-infrared region two extinction bands emerged; they peaked at 1000 and 1400 nm. We interpret these bands as due to Mie scattering from Cr precipitates. The evidence for the presence of the precipitates is derived from TEM studies.

TEM investigation of the same sample revealed the presence of Cr precipitates. These precipitates had an average size of 800 nm and had a very inhomogeneous distribution. For this reason the total concentration of the precipitates was not measured. Figure 5 shows a micrograph from one of the regions containing the highest concentration of precipitates. The rings around the precipitates were probably due to strains between the precipitates and the surrounding matrix. Selected area diffraction patterns with the beam parallel to the c axis from the largest precipitates are shown in Fig. 6. The precipitates were coherent and had a superlattice structure in the basal plane. The superlattice period was three

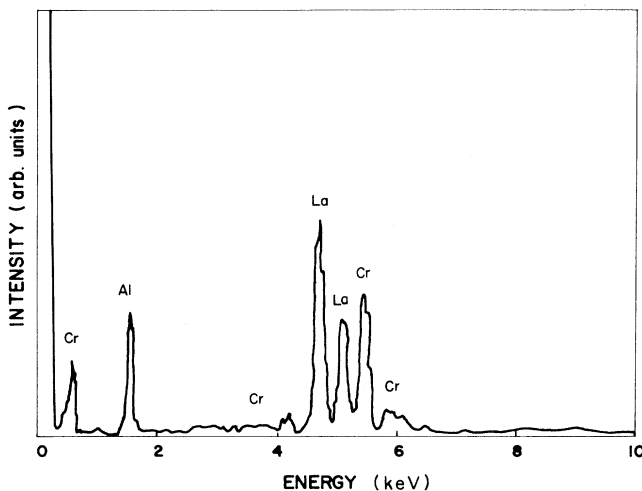


FIG. 7. X-ray fluorescence spectrum of a chromium-rich precipitate in a LMA:Cr crystal thermochemically reduced at 2020 K.

times the matrix period. The superlattice reflection were accompanied by satellite spots [Fig. 6(b)], revealing strain or small distortions in the superlattice structure. X-ray microanalysis were also performed on precipitates embedded in the matrix using the small convergent probe. Figure 7 shows a typical x-ray fluorescence spectrum from a precipitate. The corresponding Cr lines are observed. Not unexpectedly, in some cases small quantities of Cu were also detected.

The parallel optical-absorption and TEM measurements allow us to deduce that during TCR at 2020 K a large fraction of the Cr^{3+} ions had migrated to form Cr-rich precipitates.

IV. SUMMARY AND CONCLUSIONS

Chromium-doped LMA crystals have been thermochemically reduced at increasing temperatures up to 2020 K. Optical-absorption and TEM techniques were employed to monitor the presence of impurity ions, vacancies, and aggregates. The virgin sample contained no observable precipitates, and is characterized by two Cr^{3+} optical-absorption bands, which peak at 420 and 570 nm.

The results of the TCR can be roughly divided into two stages. The first stage, which began at 1500 K, was characterized by the emergence of an absorption band at 270 nm in the bulk material. This band increased rapidly with temperature. The absorption did not saturate, leading us to propose that the band was due to an intrinsic defect, most likely associated with anion vacancies. A dark coloration at the surface region also appeared during the first stage. Analytical TEM techniques determined that Cu-rich precipitates of low concentrations were present in the dark regions. Copper was not a dopant and was apparently an inherent impurity in the virgin LMA. These precipitates occasionally contained small amounts of Ti and Mo, but no chromium is present, consistent with the optical measurements, which showed that there was no loss of Cr^{3+} . As the TCR temperature increases, the dark surface layers become thicker and darker. The dark coloration is attributed to Mie scattering from the Cu-rich precipitates. In brief, we propose that during the first stage some form of anion vacancies are formed and that these vacancies lead to the formation of precipitates containing Cu, Ti, and Mo at the surface region, to the exclusion of the more dominant chromium dopant. The Cr^{3+} substitutional ions were thermally much more stable than the Cu, Ti, and Mo impurities and were not prone to aggregation in this temperature range.

The second stage primarily involved the aggregation of Cr impurities. In a reducing atmosphere and at a temperature between 1900 and 2000 K, the Cr^{3+} ions were sufficiently mobile that aggregation was possible. At a temperature of 2020 K, a significant amount of substitutional Cr^{3+} ions was lost, as monitored by the Cr^{3+} absorption bands at 420 and 570 nm, and emerged as Cr-rich precipitates. These precipitates have been identified by analytical TEM techniques. They exhibit Mie scattering, which results in extinction bands that are observed to peak at 1000 and 1400 nm.

ACKNOWLEDGMENTS

The authors would like to thank M. A. Ollacarizqueta for assistance with the x-ray microanalysis system and N. de Diego for her valuable suggestions. The transmission electron microscope work was performed at the Centro de Microscopía electrónica del Centro de Investigaciones Biológicas and at the Centro de Microscopía Electrónica de la Universidad Complutense. R.G. gratefully ac-

knowledges support from Comunidad de Madrid. This research was sponsored by the U.S. Department of Energy under Contract No. DE-AC05-84OR21400 with Martin Marietta Energy Systems, Inc. and by the U.S. Defense Advanced Research Projects Agency under Interagency Agreement No. 40-1611-85 with the U.S. Department of Energy.

*Also at U.S. Department of Energy, Division of Materials Sciences, ER131, Washington, D.C. 20585.

¹J. Narayan, Y. Chen, and R. M. Moon, *Phys. Rev. Lett.* **46**, 1491 (1981).

²M. M. Abraham, L. A. Boatner, W. H. Christie, F. A. Modine, T. Negas, R. M. Bunch, and W. Unruh, *J. Solid State Chem.* **51**, 1 (1984).

³J. Narayan, Y. Chen, R. M. Moon, and R. W. Carpenter, *Philos. Mag. A* **49**, 287 (1984).

⁴R. M. Bunch, W. P. Unruh, and M. V. Iverson *J. Appl. Phys.* **58**, 1474 (1985).

⁵C. Ballesteros, R. González, S. J. Pennycook, and Y. Chen, *Phys. Rev. B* **38**, 4231 (1988).

⁶C. Ballesteros, R. González, and Y. Chen, *Phys. Rev. B* **37**, 8008 (1988).

⁷C. Ballesteros, L. S. Cain, S. J. Pennycook, R. González, and Y. Chen, *Philos. Mag. A* **59**, 907 (1989).

⁸C. Ballesteros, R. González, Y. Chen, and M. R. Kokta (unpublished).

⁹A. E. Hughes and S. C. Jain, *Adv. Phys.* **28**, 717 (1979).

¹⁰D. Saber and A. M. Lejus, *Mater. Res. Bull.* **16**, 1325 (1981).

¹¹Kh. S. Bagdasarov, L. M. Dorozhkin, A. M. Keverkov, Yu. I. Krasilov, A. V. Potemkin, A. V. Shestakov, and I. I. Kuratev,

Kvant. Elektron. (Moscow) **10**, 1014 (1983) [*Sov. J. Quantum Electron.* **13**, 639 (1983)].

¹²D. Gourier, F. Laville, D. Vivien, and C. Valladas, *J. Solid State Chem.* **61**, 67 (1986).

¹³N. N. Mel'nik, M. N. Popova, I. T. Makhmundov, and P. A. Arsen'ev, *Fiz. Tverd. Tela (Leningrad)* **26**, 2739 (1984) [*Sov. Phys. Solid State* **26**, 1659 (1985)].

¹⁴A. K. Gerasyuk, B. V. Ignat'ev, I. I. Kuratev, V. F. Pisarenko, V. V. Popov, S. N. Shashkov, and A. V. Shestakov, *Fiz. Tverd. Tela (Leningrad)* **27**, 3136 (1985) [*Sov. Phys. Solid State* **27**, 1885 (1985)].

¹⁵V. M. Garnarsh, A. A. Kaminskii, M. I. Polyakov, S. E. Sarkisov, and A. A. Filimonov, *Phys. Status Solidi A* **75**, k111 (1983).

¹⁶C. Y. Chen, J. L. Park, L. S. Cain, G. J. Pogatshnik, M. R. Kokta, M. M. Abraham, and Y. Chen, *Phys. Rev. B* **40**, 8522 (1989).

¹⁷B. Viana, A. M. Lejus, D. Vivien, V. Ponçon, and G. Boulon, *J. Solid State Chem.* **71**, 77 (1987).

¹⁸Y. Chen, J. L. Kolopus, and W. A. Sibley, *Phys. Rev.* **186**, 865 (1969).

¹⁹Y. Chen, R. González, O. E. Schow, and G. P. Summers, *Phys. Rev. B* **27**, 1276 (1983).

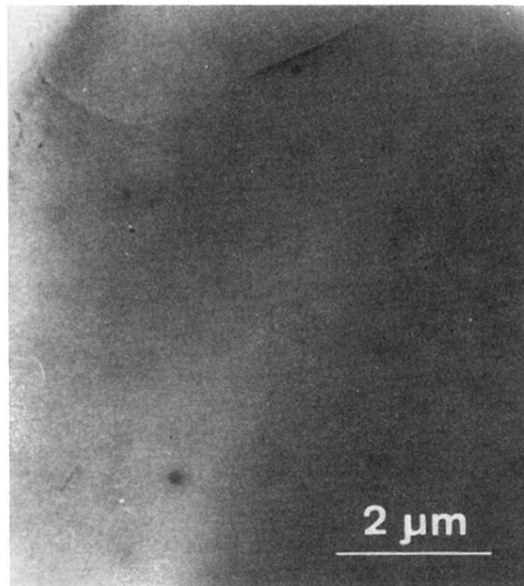


FIG. 2. Bright-field transmission-electron microscopy of precipitates in LMA:Cr crystal thermochemically reduced at 1500 K.

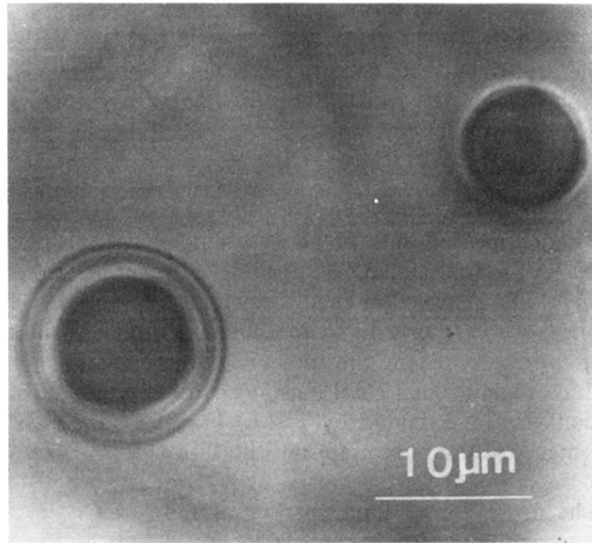


FIG. 5. Bright-field transmission-electron microscopy of precipitates in a LMA:Cr crystal thermochemically reduced at 2020 K.

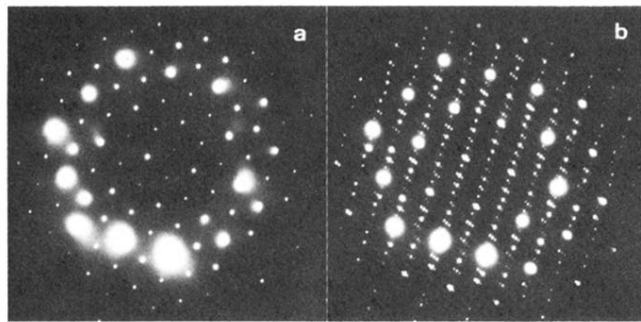


FIG. 6. Selected-area-diffraction patterns of (a) the matrix, and (b) a precipitate in a LMA:Cr crystal thermochemically reduced at 2020 K.